DIRECT OBSERVATION OF A p-τ CURVE IN A SLANT STACKED WAVEFIELD

George A. McMechan and Richard Ottolini

Abstract

The well-known Wiechert-Herglotz technique for computing a velocity-depth profile from refraction seismograms uses data in the form of ray parameter as a function of intercept time (a p-τ curve). The technique of slant stacking used by reflection seismologists automatically produces a p-τ curve from a common shot profile, thereby bypassing the arbitrary picking of traveltime and the several intermediate calculations of previous methods. Successful preliminary results are presented for both synthetic and real data. This method deteriorates for widely separated geophones and where a number of apparent sources with low inter-source coherency coexist in a single profile, but is capable of completely sorting out triplications in data with less extreme contrasts without human intervention.

Introduction

The techniques used in the processing of reflection gathers are not generally known or used by those engaged in the processing of refraction profiles. There are, however, certain essential similarities in some of the problems involved and in the parameterizations chosen in the study of those problems. Here we shall detail one salient example: the production of a ray parameter-time intercept (p-τ) curve by the

transformation of the data wavefield, or slant stacking.

Recent advances in the inversion of refraction profiles allow an envelope of possible velocity-depth profiles to be computed from an envelope in the ray parameter-offset (p-Δ) plane or in the ray parameter-time intercept (p-τ) plane. This type of operation has been variously called extremal inversion (McMechan and Wiggins, 1973) or Tau inversion (Bessonova et al., 1974; Bessonova et al., 1976; Bates and Kanasewich, 1976). One way of determining a p-τ envelope is to produce a series of reduced traveltime plots and to find the region in each where the slope is zero. This process can be shown to be equivalent to the technique of slant stacking that is used in reflection seismology. The main advantages of the slant stack approach are that it produces a complete p-τ locus by a reversible transformation of the data wavefield (i.e. the p-τ plane is a data space), that slant stacking is relatively fast, that it eliminates some of the subjectivity involved in the current methods of producing p-τ loci, that it allows explicit estimates of envelope width to be made, and that it has the added aesthetic appeal that a p-τ locus is a caustic in the transformed wavefield. (A caustic is the edge of a region of coherent energy formed by constructive interference.)

By far the most extensive application of this approach is image reconstruction in the field of nuclear medicine. A comprehensive bibliography is given by Gullberg (1979). Chapman (1978) has previously sketched some of the properties of a slant stacked refraction wavefield and referred to similar work in the field of X-ray tomography, but did not attempt to make direct application of slant stacks in inversion of refraction profiles as we do in this paper. Schultz and Claerbout (1978) have demonstrated the selectivity of slant processing in the detection of reflectors not visible in raw data so we felt it worthwhile to investigate its application to refraction data.

Connections between Refraction and Reflection

The motivation for investigating the use of reflection data processing methods with refractions is illustrated in figure 1. Figure 1a contains a sketch of a typical traveltime (T-Δ) triplication and 1b contains the corresponding p-Δ plot. Refractions are represented by prograde p-Δ branches such as 1-2, and reflections by retrograde branches such as 2-3-4.

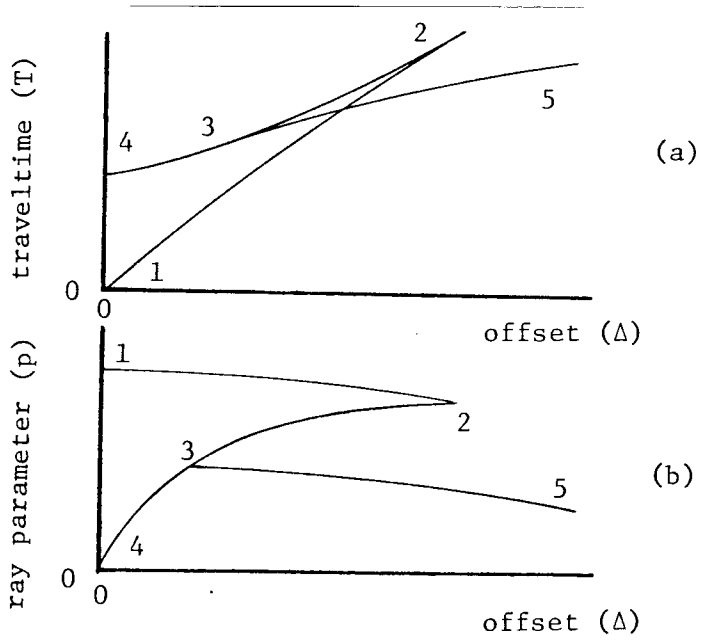

FIG. 1. The continuity of reflection and refraction branches as seen in the traveltime (a) plane and in the ray parameter (b) plane. Locus 2-3-4 is a reflection; 1-2 and 3-5 are refractions. (b) can be derived from (a) by differentiating since $p = dT/d\Delta$.

The relationships between the four variables T, Δ, p and τ are

$$T = \tau + p\Delta; \text{ and,} \tag{1}$$

$$\tau = \int \Delta \, dp \tag{2}$$

where T is traveltime, p is ray parameter, Δ is offset and τ is the traveltime projected to zero offset along a line of slope p through the

point (T,Δ). These relationships are illustrated in figure 2. This representation has been previously discussed in SEP-11 by R. Clayton. Refraction studies and velocity inversions typically involve the arrivals corresponding to the continuous locus 1-2-3-5 (figure 1). The precritical extension 3-4 is rarely specifically dealt with. One notable exception is the work of Kennett (1977) who considers loci of the type 1-2-3-4 to determine the uncertainty in the depth to a reflector.

On the other hand, studies of reflections are primarily concerned with loci such as 2-3-4 (figure 1) and ignore or even actively mask out the refraction branches 1-2 and 3-5. Note that the segment 2-3 is a region of overlap. This overlap region is included in both refraction and reflection studies but in rather different ways. The question then arises as to whether the techniques of reflection seismology may be validly and profitably applied to refraction branches and vice versa. An example of the latter was mentioned above (Kennett, 1977) and a precedent for the former is evident in the generalized ray theory described by Wiggins and Helmberger (1974) who treat the amplitude behavior of arrivals refracted by a velocity gradient in terms of reflections from a stack of thin layers. In the next section we shall exploit the treatment of a velocity gradient as the limiting case of a layered medium as the layer thicknesses go to zero.

p-τ Curves for Refraction Branches as the Envelope of p-τ Curves for Reflections

The production of a p-τ envelope from a refraction data profile is the intermediate re-parameterization usually made as preparation for Tau inversion since the Wiechert-Herglotz inversion integral can be conveniently stated as a weighted integral of a p-τ curve (Bessonova et al., 1976). A p-τ curve can be computed from a T-Δ curve or from a p-Δ curve by using equations (1) and (2) with the added observation that $p = dT/d\Delta$, as implied by equation (1). These relationships are illustrated in figure 2, which contains the T-Δ, p-Δ and p-τ representations of a model in which velocity increases slowly with depth.

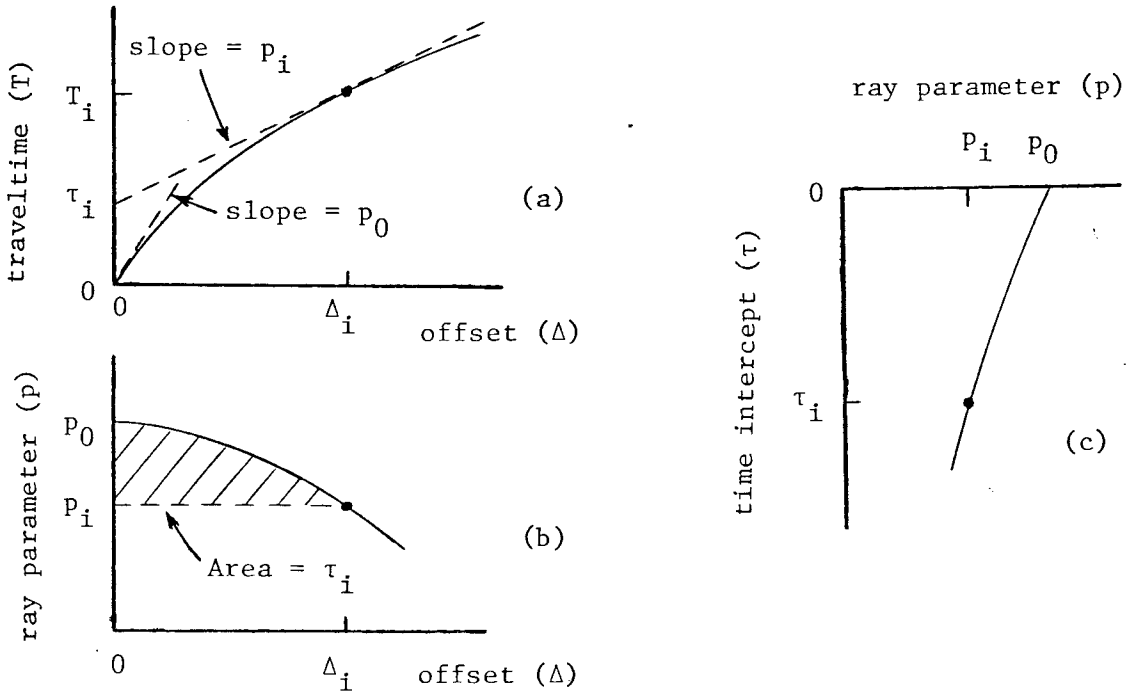

FIG. 2. The geometrical interpretation of equations (1) and (2). These curves represent a model in which arrivals are refracted by a velocity gradient. A line drawn tangent to the traveltime curve (a) at any point (T_i, Δ_i) will have slope p_i and time intercept τ_i. Thus, the traveltime curve in (a) can be mapped directly into the p-Δ plane (b) or the p-τ plane (c).

Consider how the p-τ curve in figure 2c can be expressed as the limiting case for reflections from thin layers. Figure 3 illustrates the T-Δ, p-Δ and p-τ curves for a model consisting of two constant velocity layers over a half-space in flat earth geometry. The p-τ curve in this case is completely defined in terms of the two reflected branches 2-3-4 and 5-6-7 since p and τ are fixed for all points on the refraction branches 1-2 and 6-8. Constant p implies propagation parallel to the layer boundaries and so these arrivals are more correctly termed head waves than refractions. This geometry can be extended to as many layers as desired. An example of a 15-layer model is sketched in figures 4a and 4b. The heavy line in figure 4b is the p-τ locus for Wiechert-Herglotz integration that would give back the 15-layer model.

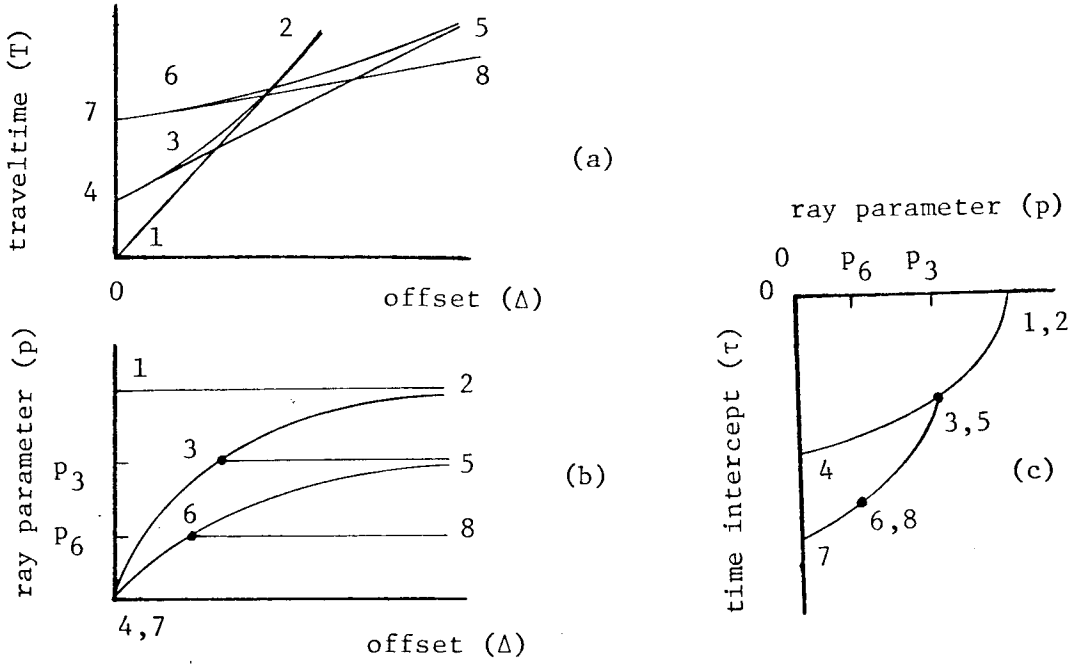

FIG. 3. The T-Δ, p-Δ and p-τ representations of a model consisting of two constant velocity layers overlying a constant velocity half-space. The numbers show the corresponding rays in each plot. Rays 1, 4 and 7 are observed at Δ = 0. Rays 3 and 6 are critical reflections.

Assume now that the layer sequences 1-6 and 8-15 in figure 4 are approximations to smooth velocity gradients and that a better approximation can be obtained by taking smaller steps. If the gradients were represented by stacks of infinitesimally thin layers, the p-τ locus would become apparently smooth as shown in figure 4c. Note that, in the limit, arrivals refracted in a velocity gradient produce convex p-τ segments and that reflections produce concave p-τ segments. In the following section methods for the production of p-τ curves from observations are discussed. Specific examples will then be presented.

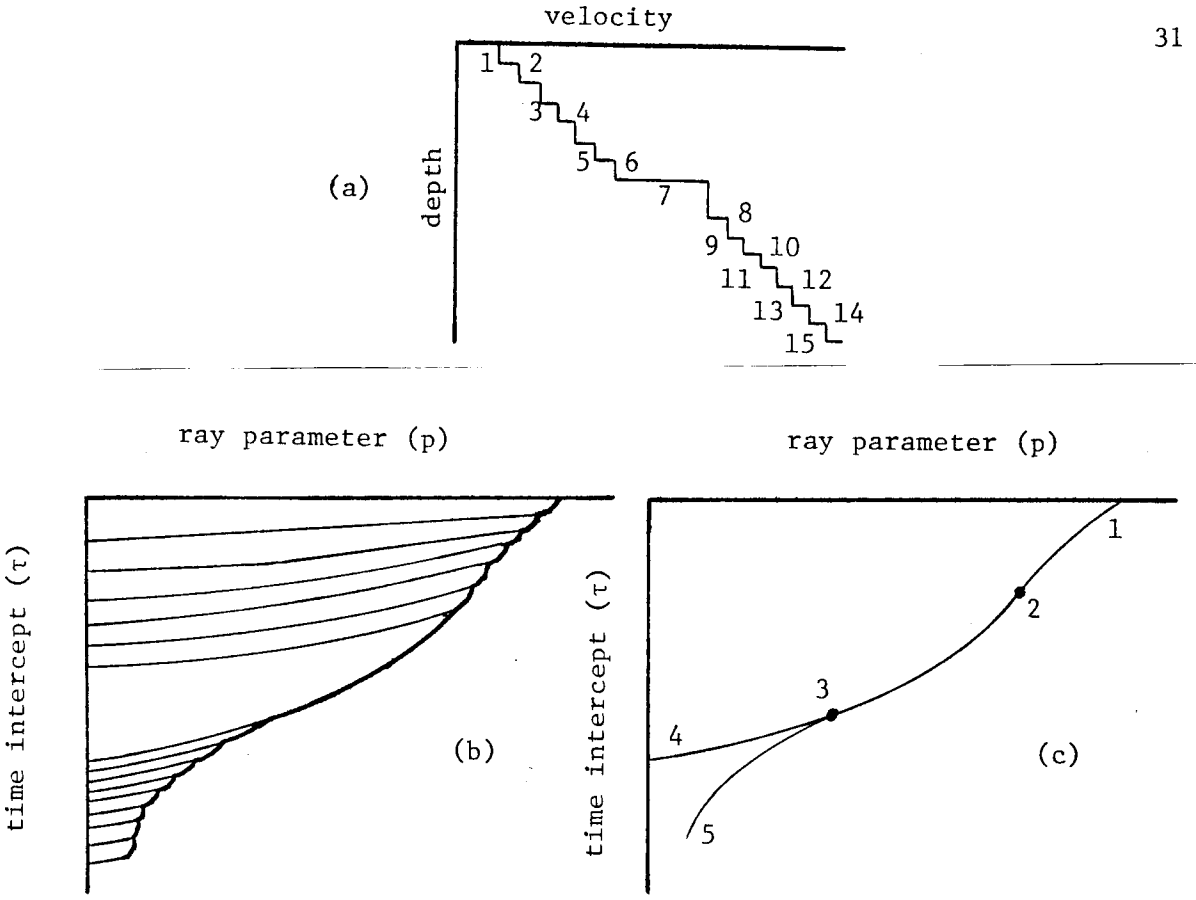

FIG. 4. The layered model in (a) can be represented in the p-τ plane as shown in (b). In (b) the heavy line is the path of integration required for Wiechert-Herglotz inversion which would give back the model in (a). As we let the layer sequences 1-6 and 8-15 approach an infinite number of thin layers, curve (b) will approach the smooth curve (c) and the steps in (a) will appear as a smooth velocity gradient. In (c) the numbered points correspond to the similarly numbered points in figure 1.

Methods of Producing p-τ Curves from Data

There are two approaches to the determination of a p-τ curve from a refraction profile - kinematic and dynamic.

The kinematic approach is the one in current use and consists of some variation of the following. The definitions of p and τ in figure 2a are not used directly for data analysis because of the difficulty of determining slopes and points of tangency from T-Δ observations that exhibit local scatter in both time and amplitude. Hence, the T-Δ curvature is enhanced by replotting the observations as a reduced time section by the transformation

$$T_R(\Delta_i, p_i) = T(\Delta_i, p_i) - p_R\Delta_i \qquad (3)$$

where $T(\Delta_i, p_i) = T_i$ is the traveltime of the point (T_i, Δ_i) ; $T_R(\Delta_i, p_i) = T_{R,i}$ is the reduced traveltime of the point (T_i, Δ_i) ; and p_R is the reduction ray parameter.

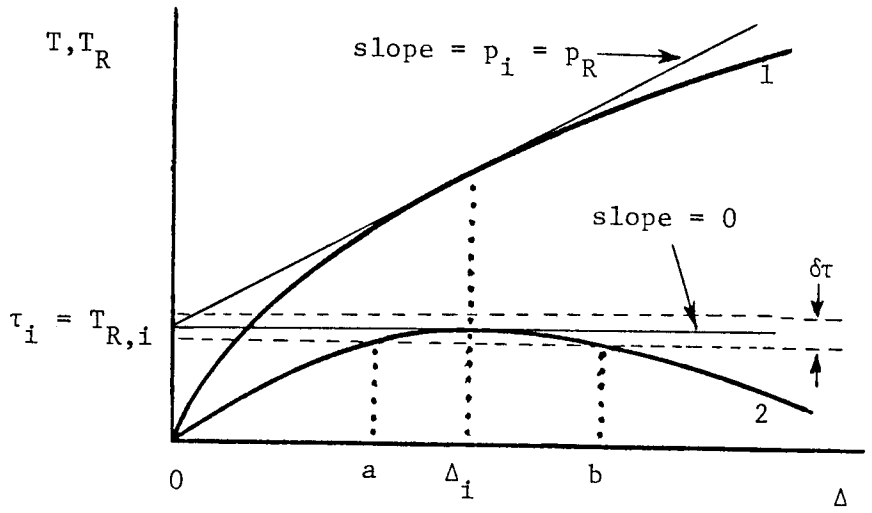

FIG. 5. The relationship between true and reduced traveltime curves. Curve 1 is the true (T) curve and 2 is the reduced (T_R) curve. A separate T_R curve is obtained for each p_R chosen. $\delta\tau$ is the uncertainty in τ at $p = p_R$ and is defined by the scatter in the data at Δ_i. The region between a and b where the T_R curve is effectively horizontal is the Fresnel zone.

The relationship between a true traveltime curve T and a reduced traveltime curve T_R is shown in figure 5. The reduced time $T_{R,i}$ corresponding to zero slope on the T_R curve is the required τ_i; the ray parameter corresponding to that point is the required p_i (= p_R); and, when a p-τ envelope as opposed to a p-τ line is being determined, the appropriate envelope width $\delta\tau$ at (τ_i, p_R) is indicated by the scatter in the reduced traveltimes. Each reduced time curve gives one point on the p-τ curve. Good examples of this procedure are illustrated by Bates and Kanasewich (1976) and Kennett (1977) among others. Variations are presented by Garmany et al. (1979) and Spudich (1979).

A major element in the philosophy which guides current state-of-the-art data processing in reflection seismology is that transformations should, whenever possible, be from one data space to another so that no data are omitted in processing at any step. Typical examples are stacking, migration and filtering. These processes all result in a new suite of seismograms (i.e., a data space), and are often reversible. On the basis of the data space criterion, p-τ, but not p-Δ, is an acceptable mode of data presentation. It is interesting in this regard that apparent velocity measurements made with arrays involve a process which is similar to slant stacking, but that the results are utilized in kinematic form (p-Δ or T-Δ); cf. Johnson, 1967; Simpson et al., 1974. A p-τ wavefield has the time dimension τ that is essential to a data space, and it can be produced from the original data traces by an inverse Radon transformation (IRT). An IRT implies an operation on the entire wavefield for all p_R, and is implemented by the procedure called slant stacking. We term this the dynamic option for producing information in p-τ space.

Slant stacking can be performed in either the time or frequency domain. In the frequency domain, the IRT, which produces a slant stack from a seismic profile, can be obtained by using the slice theorem:

$$F_{\Psi}(\omega, p) = F_{\Phi}(\omega, -\omega p) \tag{4}$$

where F_x denotes a Fourier transform of wavefield x. Φ is the observation (seismogram) wavefield and Ψ is the transformed (p-τ) wavefield. Equation (4) says that F_{Φ}, the two-dimensional Fourier transform of Φ evaluated along the line $-\omega p$, is the Fourier transform with respect to time of its projection $\Psi(\tau, p)$. In the frequency domain, a forward Radon transform (FRT) that produces a seismic profile from a slant stack is

$$\Phi(T, \Delta) = \frac{1}{4\pi^2} \int\int_{-\infty}^{+\infty} F_{\Psi}(\omega, p) \exp\left[-i\omega(T - p\Delta)\right] |\omega| \, d\omega \, dp \tag{5}$$

In the time domain, the IRT is (Gel'fand et al., 1966; Chapman, 1978;

Thorson, SEP-14)

$$\Psi(\tau, p) = \int_{-\infty}^{+\infty} \Phi(\tau + p\Delta, \Delta)\, d\Delta \qquad (6)$$

and the FRT is

$$\Phi(T, \Delta) = \int_{-\infty}^{+\infty} \Psi(T - p\Delta, p) * \left[\frac{1}{2\pi} M_{\Omega}(T - p\Delta)\right] dp \qquad (7)$$

where M_{Ω} is defined to ensure convergence of the integral (5) since the inverse Fourier transform of $|\omega|$ does not exist. Ω is a cutoff frequency which is usually set to the Nyquist frequency. A working definition of $M_{\Omega}(t)$ is

$$\Omega \frac{\sin \Omega t}{\pi t} - \frac{2 \sin^2(\Omega t/2)}{\pi t^2} = M_{\Omega}(t)$$

Slant stacking involves multiple sweeps of the data traces. Figure 6 illustrates two ways a slant stack can be done in the time domain. The first option is to fix p and sweep over τ; the second is to fix τ and sweep over p and then to increment the fixed quantity and repeat the sweep. In either case the procedure is to sum all the amplitudes along a given line of slope p and intercept τ and to plot that accumulated amplitude in the new p-τ data space. The transformed wavefield has a sample increment of $d\tau$ in time and its traces are separated from each other by the p increment dp (see figure 9 for an example). dp is chosen to be < a Fresnel zone, which is that increment corresponding to the region of apparently constant p (figure 5).

Figure 7 illustrates a third way of performing slant stacking in the time domain, that is, from the point of view of the total contribution of a single arrival. Each T-Δ point contributes along a locus in the p-τ plane that goes from $(p, \tau) = (+\infty, -\infty)$ to $(-\infty, +\infty)$ as shown in

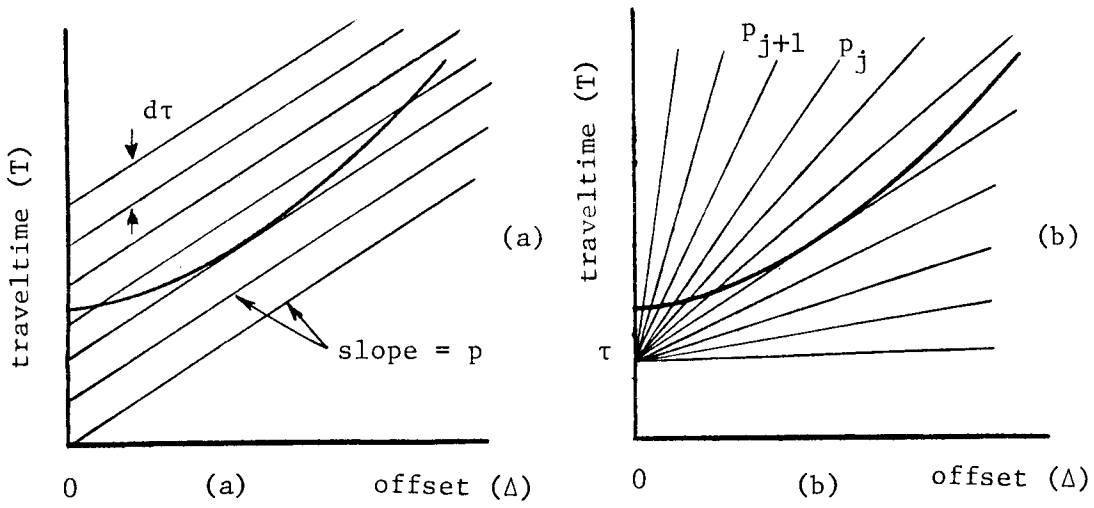

FIG. 6. Two methods of performing a slant stack. The heavy lines are the traveltime curves. In (a) the ray parameter is fixed and τ is incremented. In (b) τ is fixed and the slope p is incremented. $dp = p_{j-1} - p_j$ where j is arbitrary.

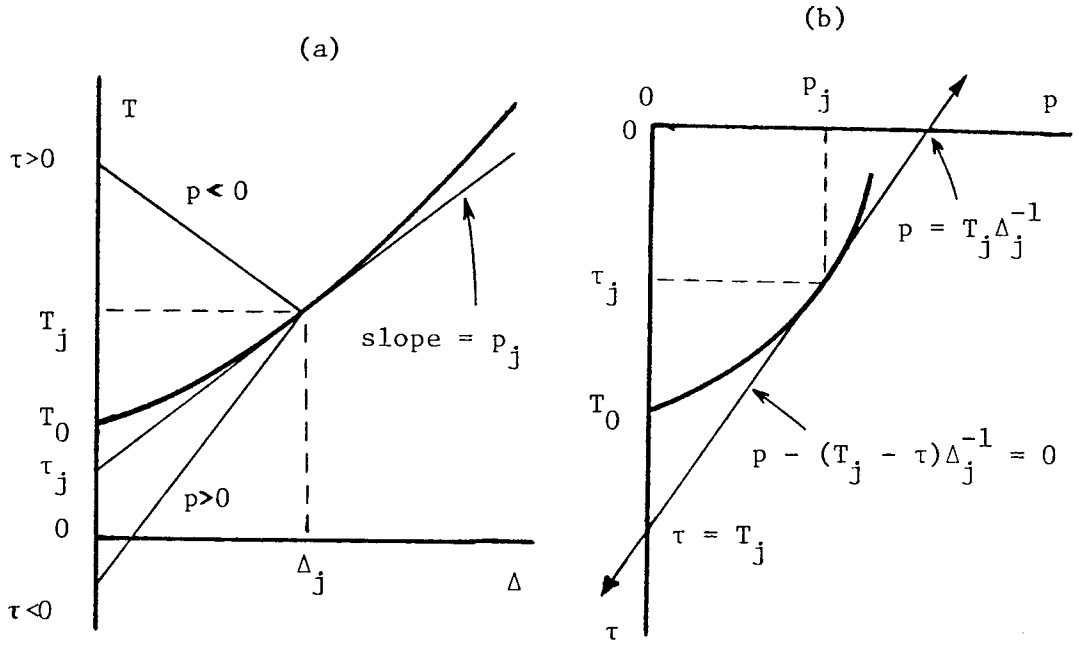

FIG. 7. A single arrival (T_j, Δ_j) in the T-Δ plane transforms onto a line $p = (T_j - \tau)/\Delta_j$ in the p-τ plane. The heavy line in (a) is the T-Δ curve; the heavy line in (b) is the corresponding p-τ curve. The operation to get from (a) to (b) is typically thought of as mapping in the kinematic approach, but is viewed via the dynamic (wavefield) approach as a transformation.

figure 7b. Each such locus is a straight line as it is an alternate expression of equation (1):

$$p = (T - \tau)\Delta^{-1} \tag{8}$$

The maximum integrated amplitude contribution for the point (T_j, Δ_j) will occur at the point (p_j, τ_j) in the p-τ plane (figure 7b) because of constructive interference with the arrivals within the increment $p_j+\varepsilon$ and $p_j-\varepsilon$ where ε is the half-width of the Fresnel zone (figure 5). Thus, the locus of (p_j, τ_j) in a slant stacked wavefield appears as a caustic curve. Examples are presented below.

A single seismogram, which is a locus of constant Δ in the T-Δ plane, transforms onto the entire family of straight lines of slope $-1/\Delta$ in the p-Δ plane since, from equation (8):

$$\frac{dp}{d\tau} = -\Delta^{-1} \tag{9}$$

which can be recognized as a statement of the solution of Clairaut's equation (Ince, 1956). Chapman (1978) has exploited this property for the construction of synthetic seismograms from a p-τ curve. The major contributions to a seismogram at any Δ come from those elements in the p-τ plane where there is significant energy with slope $-1/\Delta$. This can be recognized as the FRT as defined by equation (7). Thus, we have obtained in an intuitive way the underlying principle of the work of Chapman (1978) and Wiggins (1976), as expressed in equation (5), by approaching it from the direction of the slant stack processing of seismic reflection data.

It should be noted that, provided that a sufficiently small dp is chosen, slant stacking does not involve any restricting assumptions about the data. It is simply an alternate and equivalent form of data presentation. Thus, for example, if one can construct a p-τ curve for a laterally inhomogeneous medium, a profile of seismograms is defined, but the physical validity of this profile is questionable because p changes along the ray when the incident angle is no longer referenced to

vertical. Other practical model-independent applications are, however, possible. For example, interpolation to produce a seismogram at any desired Δ in a recorded or synthetic profile can be done by doing an IRT of the available traces, and then an FRT for the desired value of $-1/\Delta$. Radon transforms can also be used to filter a complete profile at once since noise tends to stack at the higher p values. Both interpolation and filtering have been found to work well, but these applications are beyond the scope of the present paper and so will be reported elsewhere in more detail.

To this point most of what we have presented is not new. The application to which we now turn, however, is new; the foregoing sections were included for completeness and to set the stage for the examples in the following section. Also, since the sources for the theoretical foundation of our work are not available in any one other publication we have attempted to give a fairly complete synthesis of the salient ideas.

Examples

In order to illustrate the properties of slant stacks of refraction profiles two refraction profiles, one synthetic and one real, were processed. Each of these will be presented in turn.

The synthetic example was derived from the p-Δ curve shown in figure 8. A synthetic refraction seismogram profile produced from this p-Δ curve by the disk ray theory algorithm (which is a form of FRT) of Wiggins (1976) was slant stacked to produce the wavefield in figure 9a. A discussion and examples of the disk ray theory algorithm was also presented by R. Clayton in SEP-11. In figure 9a many of the individual linear loci described above (figure 7) can be followed and seen to combine to form a high amplitude caustic as predicted by the theory. This caustic should be the desired p-τ curve. For comparison, the p-τ curve computed directly from the p-Δ curve in figure 8 by equation 1c is shown in figure 9b. Because slant stacking induces a time-stretching of the data, a filter which enhances the higher frequences is a useful compensatory step and has been applied in obtaining figure 9a. For comparison,

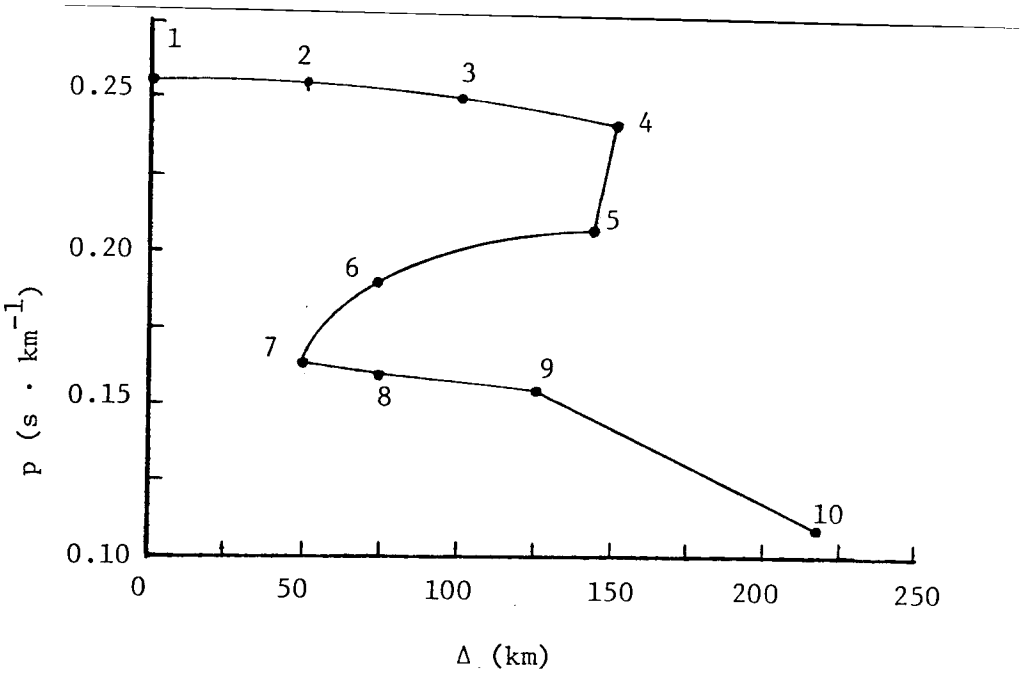

FIG. 8. A model p-Δ curve. This curve was used to construct a theoretical example of refraction slant stacks as discussed in the text.

the unfiltered results are shown in figure 9c.

Before considering a real data example it is important to emphasize the salient criteria and sources of potential difficulty in correct identification of the desired p-τ locus. The most important point is the perceptual paradox that, although an entire slant stack wavefield is composed of straight lines, one should avoid seeing them. This may take some practice but it is essential since the goal is to find a continuous (except where a low velocity zone occurs), piecewise curved caustic which is the envelope of the straight lines. In a slant stack wavefield, continuity of the p-τ locus corresponding to a T-Δ triplication is expected because the initial motions of both refractions and postcritical reflections are in the same direction. Precritical reflections are phase shifted by an amount which approaches π relative to the postcritical reflections, and so they exhibit an apparent disconnection from the main p-τ locus near the critical reflection.

FIG. 9. Slant stacks for a synthetic refraction profile. The synthetic profile from which these slant stacks were produced was computed from the p-Δ curve in figure 8. The numbers along the curve in (b) correspond to the similarly numbered points along the p-Δ curve in figure 8. The curve (b) was produced by direct integration of the p-Δ curve in figure 8 and can be used as a basis for comparison. The inflection points (4 and 7) correspond to the cusps on the p-Δ curve. Stacks (a) and (c) were produced from the same synthetic profile. Stack (a) included a filter to enhance high frequencies; stack (c) did not. Curve (b) is displaced in τ relative to (a) by 10 sec.; (c) is displaced by 20 sec.

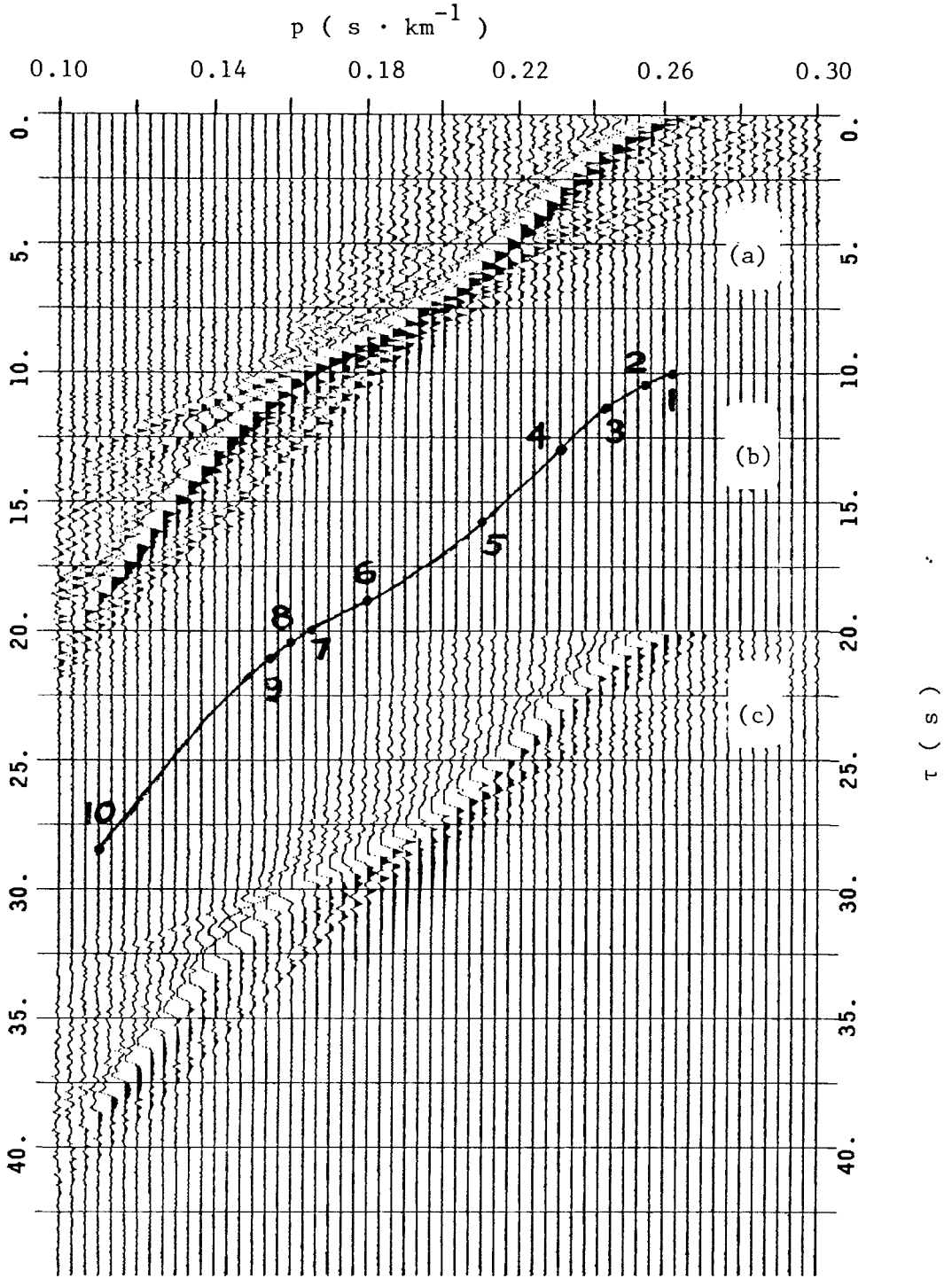

Even with the best of deconvolutions, any given arrival in a profile can rarely be confined to one cycle, and if it can it is usually at the expense of other arrivals. There are, therefore, in a slant stack, extensions from the desired p-τ locus toward greater τ which can be recognized and eliminated from consideration. Additionally, while the caustic is often associated with the largest amplitude in the local region of the wavefield, this is not a stable guide, especially when seismograms from different sources have been combined into one profile.

It is useful when ambiguities are present to plot the slant stack with a variety of formats (e.g. polarity reversal) and with various filters, to aid in accurate location of the caustic. The caustic itself should remain in a fixed position and correspond to zero amplitude throughout these changes. For example, compare figures 9a and 9c. In 9a, the caustic is simply locatable by searching between the maximum positive and maximum negative amplitudes at each p. In figure 9c, the first polarity change as τ increases is a useful criterion.

In summary, the key features of the p-τ locus are continuity, curvature and minimum τ. With these points in mind the investigation of the slant stacks of a real dataset can proceed.

Figure 10a contains a reproduction of a common shot refraction profile that was first presented by Richards and Walker (1959) and was interpreted by Richards (1960). Grant and West (1965) presented the results of Richards (1960) directly, not attempting reinterpretation. On the basis of the results of slant stacking these data we have produced a p-τ curve which differs only minutely from the interpretation of Richards (1960), who used classical kinematic techniques. The only difference between the interpretations is that we find slight velocity gradients, whereas Richards assumed constant velocity layers. For example, Richards himself noted that the refraction labeled in figure 10a seems not to be tangent to the reflection branch at the critical distance and suggested that this may be due to difficulty in observing the first cycle of the refracted arrivals. An alternative explanation is that there could be a velocity gradient at the top of the main reflector, which is the Rundle limestone.

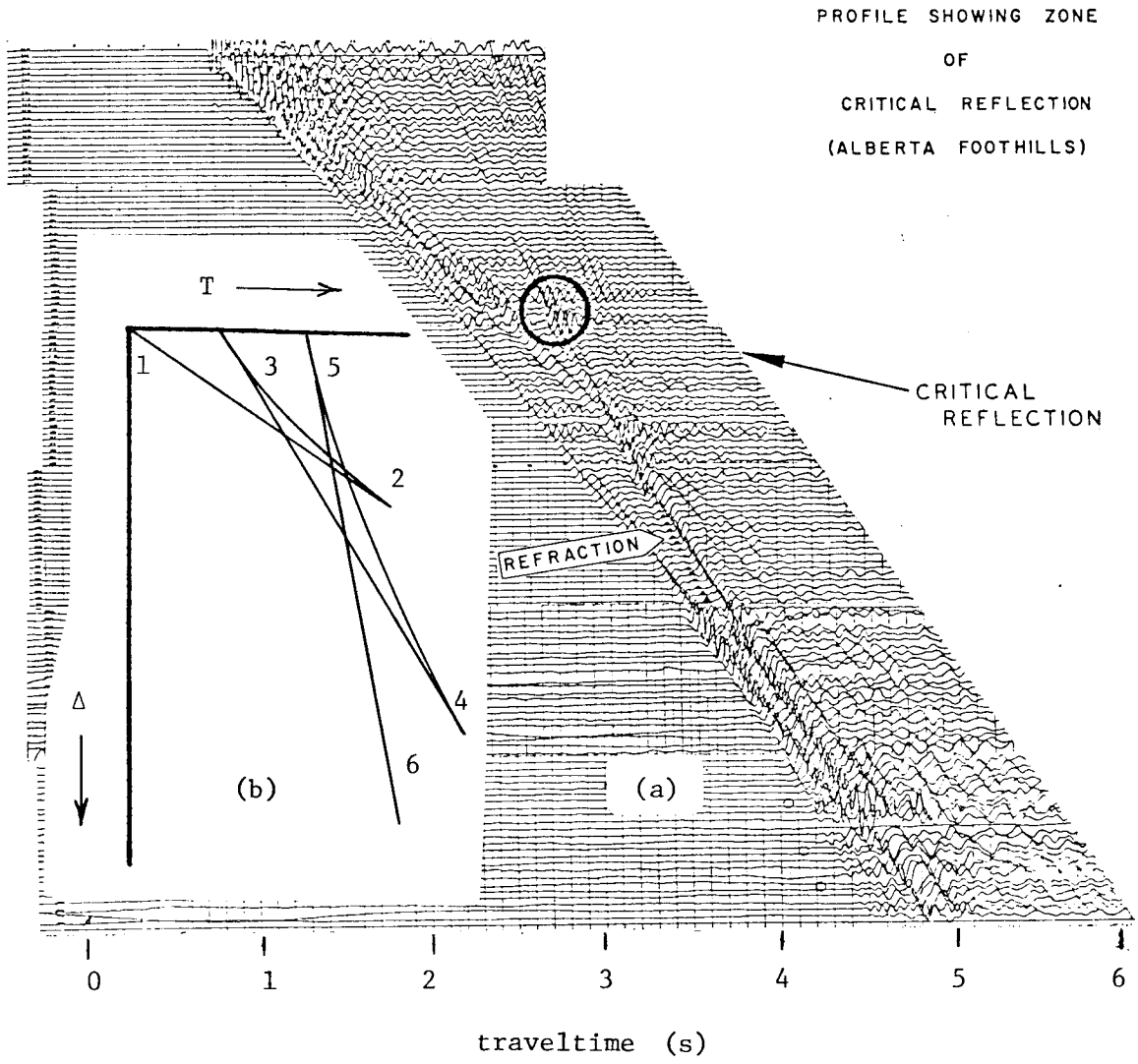

FIG. 10. The refraction profile in (a) is reproduced from Richards (1960). The first (upper) trace is at Δ = 7450 feet from the shot point and the spacing between traces is 400 feet. Six shot sizes ranging from 30 to 175 lbs were recorded. The digitization required for slant stacking unavoidably introduced some high frequency noise. Two slant stacks of these data are shown in figure 11. The insert (b) shows a sketch of the interpretation indicated by the slant stacks. The path indicated by increasing numbers is a path of constantly decreasing p. The same path is shown in figure 11c. This sketch has been purposely distorted in order to make each branch clearly visible.

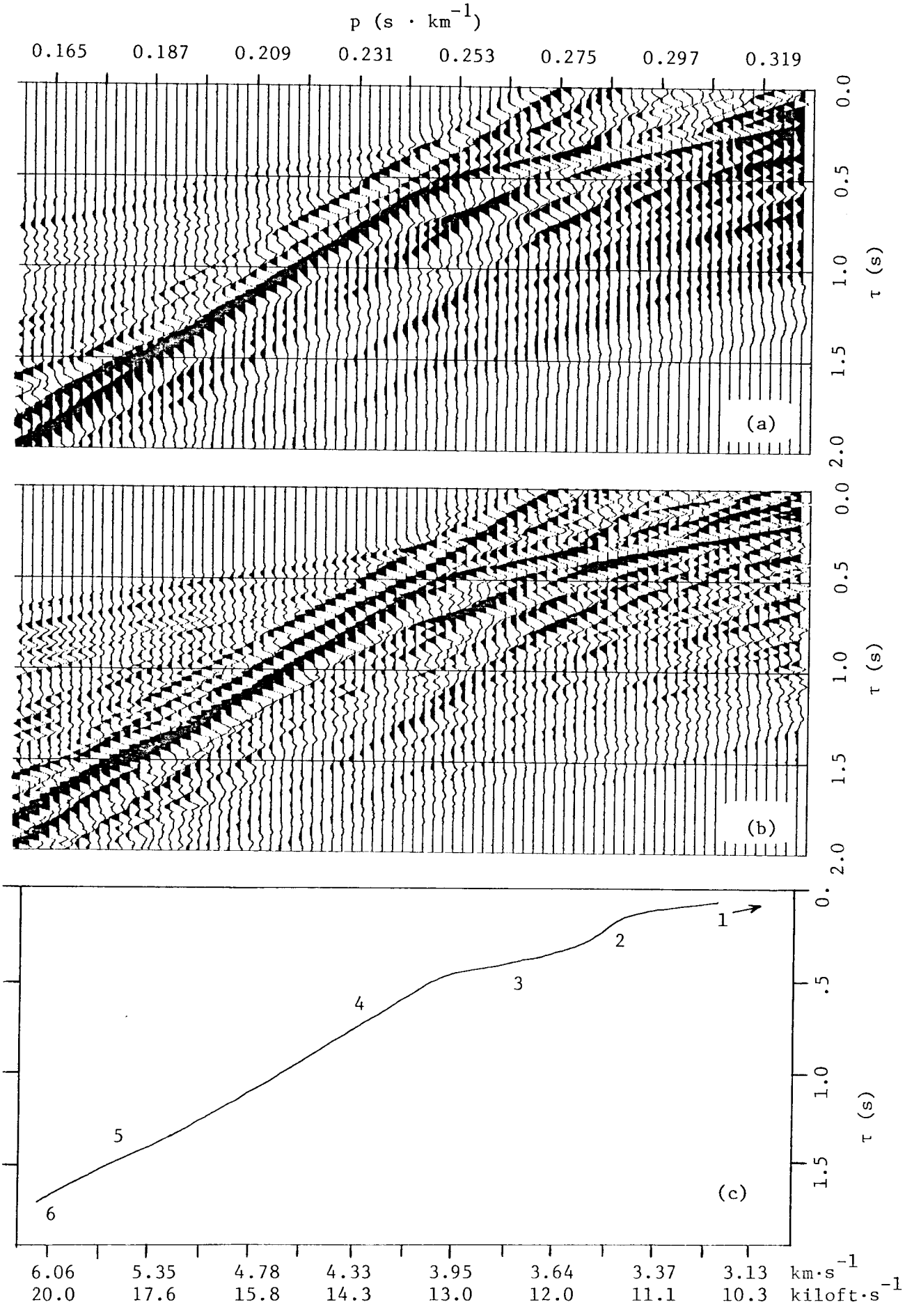
p (s · km^{-1})
0.165
0.187
0.209
0.231
0.253
0.275
0.297
0.319
0.0
0.5
1.0
1.5
2.0
τ (s)
(a)
(b)
(c)
1
2
3
4
5
6
6.06
5.35
4.78
4.33
3.95
3.64
3.37
3.13
km·s^{-1}
20.0
17.6
15.8
14.3
13.0
12.0
11.1
10.3
kiloft·s^{-1}
apparent velocity

FIG. 11. Slant stacks for the refraction profile in figure 10a. Stack (a) is the unfiltered stack, (b) is similar to (a) but includes high frequency enhancement filtering, and (c) is the net result which is the p-τ locus extracted from (a) and (b). The numbers in (c) correspond to those in the sketch in figure 10b. We present the extra velocity scale in kilofeet / sec. for those readers who wish to make a comparison with the results of Richards (1960).

Figure 11 contains the results of slant stacking the profile in figure 10a. Two stacks are shown, one unfiltered (a) and one filtered (b) as was done in figure 9. The p-τ curve that was extracted is contained in figure 11c. The p-τ locus is not complete right up to $\tau = 0$ because the data do not include traces at the smaller distances (figure 10a). As the apparent velocity decreases, the high frequency content of the arrivals generally increases (figure 10a), so at small τ the p-τ locus is more clearly seen in the filtered stack in figure 11b than in the unfiltered stack in figure 11a.

In choosing the profile in figure 10a we sought an example upon which to test the slant stack procedure through a duplication of previously obtained results. Our results support the basic interpretation originally proposed by Richards (1960) so we feel that further application and investigation of slant stacking for use in refraction interpretation is warranted. Of particular interest would be application to profiles containing ambiguities since the work of Schultz and Claerbout (1978) indicates that a high level of selectivity is associated with slant processing.

Further Comments

Although the concept of slant stacking is straightforward, there are a number of limitations and computational complications in practical application. These can be salient determinants of the success or failure of specific applications, so some mention of the main ones is in order at this point.

One of the main limitations for the application of slant stacking to refraction profiles arises from the fact that the profiles are usually spatially aliased. In order to avoid spatial aliasing the geophones must be placed at a distance from each other which is less than one-half the wavelength of the highest frequency one wishes to resolve; aliasing is thus increasingly more important as Δ decreases. An aliased profile does not allow a reliable p-τ locus to be produced since it is essentially a series of independent points, each of which produces end effects (see below).

Another limitation associated with data is related to the inter-source coherency of the apparent source functions in the data. This is no problem when the sources are shots but might be a problem if earthquake sources were used. Since slant stacking depends upon constructive interference to delineate the p-τ locus it works well only when the apparent sources exhibit the same initial polarity. For the purpose of p-τ determination the length of apparent source functions is not critical, nor is their similarity beyond the first half cycle. In fact, dissimilarity in the later parts of the wavetrain is an advantage because these will not then contribute potentially confusing coherent streaks in the p-τ plane.

Another feature to be aware of is the end effects due to spatial data truncation. End effects are seen in the p-τ plane as a fan of energy passing through the p-τ point corresponding to the end of a truncated T-Δ branch. Examples are shown by Schultz and Claerbout (1978). End effects can be reduced by extrapolating the data wavefield prior to stacking or by employing tapered mutes.

The stacking algorithm itself produces a smearing of energy toward the direction of increasing τ. A clear example of this is seen in figure 9c. The smearing is predictable, however, and hence can be eliminated by filtering. For a forward slant stack, smearing toward increasing τ is not important since it is the locus of minimum coherent τ that is desired. Smearing is important if reverse stacking is to be done because smearing in the direction of decreasing τ gives the seismograms an unwanted acausal component.

One of the main computational elements required in slant stacking is a stable interpolation scheme. This is evident if one considers the time-domain form of slant stacking [equation (6)] by which amplitudes are summed along lines that pass obliquely through a wavefield that is sampled at some fixed time increment. In the frequency domain approach [equation (4)] interpolations are required in ωp.

There are a number of options that can be programmed. For example, if one has prior knowledge of the approximate location of a traveltime curve, or if a particular branch requires detailed study, mutes can be

applied to the data to reduce unwanted contributions. These mutes are typically tapered to avoid introduction of truncation or end effects. More complete discussions of the advantages and difficulties in practical slant stacking will be presented elsewhere by the second author.

One can speculate on the potential application of slant stacking to the automation of refraction inversions. We have here demonstrated that, providing that the data meets certain criteria, the p-τ curve can be directly obtained. All that is required in addition is an algorithm that will search out the p-τ locus or envelope in the slant stacked wavefield to input into a standard inversion program. We have already mentioned a couple of overly simplistic criteria for p-τ locating. Additional constraints, such as requiring a monotonically decreasing function of both p and τ, or the tighter constraint of requiring a final model to be a single valued velocity function of depth, are obvious. Pattern recognition algorithms are usually cumbersome and it may be desirable to retain some human intervention and intuition in the inversion process. When presented as a slant stacked wavefield, the absolute maximum $\delta\tau$ at any p is one period of the wavefield local to the p-τ point in question, and a $\delta\tau$ of the order of one tenth of a period would be realistic for most visually determined envelopes.

A potential application for an automated inversion scheme is to marine profiles. Present marine recording cable configurations typically involve 48 or 96 channels and well-known sources, but their geometry tends to favor long recording times as opposed to a wide range in Δ, so that complete triplications are rarely recorded. The use of longer recording cables could produce ideal datasets for automated inversion. Another marine option which would allow extended distances would be a fixed (perhaps ocean bottom) recorder used with a moving repetitive source.

Conclusion

The application of slant stacking to the processing of refraction profiles has been demonstrated. Providing that certain criteria with respect to data quality, spacing and Δ extent are met, slant stacking is

capable of unfolding triplications. These preliminary results encourage further application and development toward realizing the demonstrated potential of the routine processing of some types of refraction profile in a highly automated manner.

ACKNOWLEDGMENTS

During the course of this project one of the authors (G.M.) was on leave at the Stanford Exploration Project, Department of Geophysics, Stanford University, which provided superb computing facilities and more than ample motivation. Critical reviews of the paper by R. Clayton, W. Mooney, R. Stolt, R. Geller, D. Weichert and D. Hill were much appreciated.

REFERENCES

Bates, A.C., and Kanasewich, E.R., 1976, Inversion of seismic traveltimes using the Tau method: Geophys. J., v. 47, p. 59-72.

Bessonova, E.N., Fishman, V.M., Ryaboyi, V.Z., and Sitnikova, G.A., 1974, The Tau method for inversion of traveltimes -I. Deep seismic sounding data: Geophys. J., v. 36, p. 377-398.

Bessonova, E.N., Fishman, V.M., Shnirman, M.G., Sitnikova, G.A., and Johnson, L.R., 1976, The Tau method for inversion of traveltimes -II. Earthquake data: Geophys. J., v. 46, p. 87-108.

Chapman, C.H., 1978, A new method for computing synthetic seismograms: Geophys. J., v. 54, p. 481-518.

Garmany, J., Orcutt, J.A., and Parker, R.L., 1979, Traveltime inversion - A geometrical approach: J. Geophys. Res., v. 84, p. 3615-3622.

Gel'fand, I.M., Graev, M.I., and Vilenkin, N.Ya., 1966, Generalized functions, Vol. 5, Integral geometry and representation theory: New York, Academic Press.

Grant, F.S., and West, G.F., 1965, Interpretation theory in applied geophysics: New York, McGraw-Hill.

Gullberg, G.T., 1979, The attenuated Radon transform - Theory and application in medicine and biology: Ph.D. Thesis, Lawrence Berkeley Lab., University of California.

Ince, E.L., 1956, Ordinary differential equations: New York, Dover.

Johnson, L.R., 1967, Array measurements of P velocities in the upper mantle: J. Geophys. Res., v. 72, p. 6309-6325.

Kennett, B.L.N., 1977, Inversion of reflected wave traveltimes: Geophys. J., v. 49, p. 739-746.

McMechan, G.A., and Wiggins, R.A., 1972, Depth limits in body wave inversions: Geophys. J., v. 28, p. 459-473.

Richards, T.C., 1960, Wide angle reflections and their application to

finding limestone structures in the foothills of western Canada: Geophysics, v. 25, p. 385-407.

Richards, T.C., and Walker, D.J., 1959, Measurement of the thickness of the Earth's crust in the Albertan plains of western Canada: Geophysics, v. 24, p. 262-284.

Schultz, P.S., and Claerbout, J.F., 1978, Velocity estimation and downward continuation by wavefront synthesis: Geophysics, v. 43, p. 691-714.

Simpson, D.W., Mereu, R.F., and King, D.W., 1974, An array study of P-wave velocities in the upper mantle transition zone beneath northeastern Australia: SSA Bull., v. 64, p. 1757-1788.

Spudich, P.A., 1979, Oceanic crustal studies using waveform analysis and shear waves: Ph.D. Thesis, San Diego, University of California.

Wiggins, R.A., 1976, Body wave amplitude calculations -II: Geophys. J., v. 46, p. 1-10.

Wiggins, R.A., and Helmberger, D.V., 1974, Synthetic seismogram computation by expansion in generalized rays: Geophys. J., v. 37, p. 73-90.